JBAT 14(2) (2025) 82 – 95

Jurnal Bahan Alam Terbarukan

Accredited SINTA 3 by Ministry of Research and Technology/National Research and Innovation Agency
SK No. 10/C/C3/DT.05.00/2025
http://journal.unnes.ac.id/nju/index.php/jbat

p-ISSN 2303 0623
e-ISSN 2407 2370

Thermodynamic Modelling of Phenolic Compound Extraction from Bio-Oil Derived from Multi-Feedstock Biomass Pyrolysis

Alifyan Syauqi✉, Dewi Selvia Fardhyanti, Haniif Prasetiawan

DOI: https://doi.org/10.15294/jbat.v14i2.40030

Chemical Engineering Department, Faculty of Engineering, Universitas Negeri Semarang, UNNES Kampus Sekaran, Gunungpati, Semarang, 50229 Indonesia

Article Info

Article history:
Received
15 August 2025
Revised
30 October 2025
Accepted
27 November 2025
Published
December 2025

Keywords:
Bio-oil;
NRTL;
Thermodynamic modeling;
Extraction temperature;
UNIFAC, UNIQUAC

Abstract

Biomass exhibits substantial potential as a renewable energy source in the form of bio-oil; however, further upgrading is required, including the separation of phenolic compounds through liquid–liquid extraction (LLE). Previous studies on LLE modelling of bio-oil have explored variations in feedstock type, pyrolysis temperature, extraction temperature, solvent selection, and thermodynamic models. This study focuses on thermodynamic modelling of phenol extraction from bio-oil derived from the pyrolysis of mixed biomass using the NRTL, UNIQUAC, and UNIFAC models. The objectives are to evaluate the influence of extraction temperature and to identify the most suitable thermodynamic model for phenol extraction from bio-oil produced by mixed biomass waste pyrolyzed at 500 °C. The results demonstrate that extraction temperature significantly influences the LLE behaviour of phenol extraction from mixed biomass waste bio-oil across all evaluated models. Correlation analysis and root mean square deviation (RMSD) values indicate that the NRTL model provides the best predictive performance, particularly at an extraction temperature of 40 °C. Furthermore, the NRTL model is identified as the most appropriate thermodynamic model for predicting phenol extraction from bio-oil produced by the pyrolysis of mixed biomass waste at 500 °C. This superior performance is attributed to the NRTL model's capability to accurately represent liquid–liquid equilibrium in both binary and multicomponent systems, especially under dilute conditions, outperforming the UNIQUAC and UNIFAC models.

INTRODUCTION

Indonesia is a developing country that experiences continuous population growth each year. In 2023, Indonesia's current population is 281,190,067, with a projected increase of 14% to 320,712,949 by 2050 (Statistics, 2023). Population growth inevitably leads to an increase in energy demand (Prastika, 2023). However, public dependence on fossil energy remains significantly higher compared to the utilization of renewable energy sources (Hertadi et al., 2022). As of 2021, the Ministry of Energy and Mineral Resources (ESDM) reported that 65.30% of domestic electricity production was still generated by coal-fired power plants (CFPPs). Over the past decade, crude oil production in Indonesia has shown a declining trend, decreasing from approximately 315 million barrels (862 thousand barrels per day) in 2012 to around 240 million barrels (659 thousand barrels per day) in 2021. This decline is primarily attributed to the aging of major oil production wells, while the contribution from newly developed wells remains limited (Lestari et al., 2021). Therefore, collective efforts are required to accelerate the development of renewable energy sources (RES) (Logayah et al., 2023). Various types of renewable energy can be implemented, indicating a high potential for renewable energy to replace fossil fuels (Fathahillah et al., 2022).

✉ Corresponding author:
E-mail: dewiselvia@mail.unnes.ac.id

Bio-oil is one of the renewable energy sources that offers a promising solution to the depletion of fossil fuel resources (Yudhistira & Wibowo, 2022). Bio-oil can be produced through the pyrolysis of biomass (Febriyanti et al., 2019). Biomass is readily available, has significant potential as a renewable energy source, and is considered carbon-neutral (Gufron et al., 2023). Agricultural biomass waste is commonly utilized as animal feed; however, when unused, it is often openly burned, contributing to environmental pollution (Putri et al., 2023). According to data from the Indonesian Central Statistics Agency, rice production in Indonesia reached 31.36 million tons in 2021, while plantation sectors such as oil palm, rubber, and others generated approximately 54.66 million tons of biomass waste.

To be utilized as a renewable fuel source in the form of bio-oil, biomass must undergo several processing steps. Pyrolysis has been identified as a more efficient and environmentally friendly method for converting biomass into bio-oil compared to other processing techniques (Kumar et al., 2020). Bio-oil is a liquid fuel derived from the thermal conversion of organic materials and is therefore classified as an environmentally friendly renewable energy source (Putri & Nurisman, 2019). Previous studies have reported the production of bio-oil from various biomass feedstocks, including rice husk (Fardhyanti, Chafidz, et al., 2020), coconut shell (Fardhyanti et al., 2018), sugarcane bagasse (Ordonez-Loza et al., 2021), empty palm oil fruit bunches (Dolah et al., 2021), spent coffee grounds (Mora-Villalobos et al., 2023), corn cobs (Fardhyanti, Imani, et al., 2020), banana peels (López et al., 2021), and orange peels (Zhu et al., 2021). Most of these studies employed single-feedstock biomass for bio-oil production via pyrolysis.

Bio-oil produced from the pyrolysis of rice husk at temperatures of 500 °C and 600 °C contains phenolic compounds of 16.42% and 31.66%, respectively (Fardhyanti, Chafidz, et al., 2020). Liquid–liquid extraction (LLE) is commonly used to separate phenolic compounds from bio-oil. Numerous studies have investigated liquid–liquid equilibrium (LLE) modeling of bio-oil systems using different feedstocks, pyrolysis temperatures, extraction temperatures, solvents, and equilibrium models. However, studies examining the effect of multi-feedstock biomass composition remain limited. The use of multi-feedstock biomass is expected to enable the utilization of diverse biomass resources with varying qualities, thereby contributing to biomass waste reduction.

Despite extensive studies on liquid–liquid equilibrium (LLE) modeling of phenolic compound extraction from bio-oil, most existing research has primarily focused on single-feedstock biomass, with variations limited to pyrolysis temperature, extraction conditions, solvent selection, or thermodynamic models. The influence of multi-feedstock biomass composition on phase equilibrium behavior, activity coefficients, and model accuracy has received limited systematic investigation, even though industrial-scale bio-oil production commonly involves heterogeneous biomass mixtures. Furthermore, comparative evaluations of local-composition models (NRTL and UNIQUAC) and group-contribution models (UNIFAC) under identical experimental conditions remain scarce, particularly for polar–nonpolar multicomponent systems relevant to phenol extraction.

Therefore, this study provides a novel contribution by systematically investigating the liquid–liquid equilibrium behavior of phenol extraction from bio-oil derived from mixed biomass feedstocks produced via pyrolysis at 500 °C, using methanol–chloroform solvent systems. The novelty of this work lies in the integration of experimental LLE data with comprehensive thermodynamic modeling, including activity coefficient analysis, RMSD-based model validation, and temperature-dependent performance comparison of the NRTL, UNIQUAC, and UNIFAC models. The findings offer quantitative insight into the effect of extraction temperature on model accuracy, identify the most suitable thermodynamic model for multi-feedstock bio-oil systems, and provide a reliable foundation for process design, scale-up, and equilibrium prediction in bio-oil upgrading applications.

Therefore, this study focuses on the liquid–liquid equilibrium modeling of phenol extraction from bio-oil produced by the pyrolysis of mixed biomass feedstocks, using the NRTL, UNIQUAC, and UNIFAC thermodynamic models.

MATERIALS AND METHOD

Materials

Biomasses waste material used in this study were oil palm empty fruit bunch obtained from the Sumatra, Sugarcane bagasse obtained

from the forestry in Jawa Timur and sawdust obtained from the local sawmill at Gunungpati. The chemicals used in this study were Methanol (≥99.8%, analytical grade, Merck, Germany) and chloroform (≥99.5%, analytical grade, Merck, Germany) were used as extraction solvents.

Method

Pyrolysis Process

Wood sawdust, oil palm empty fruit bunches (EFB), and sugarcane bagasse were first dried and sieved using a sieve shaker to obtain a uniform particle size of 60 mesh. The biomass materials were then mixed according to the following composition: 36.64 wt% EFB, 32.82 wt% sugarcane bagasse, and 30.54 wt% wood sawdust. A total of 1000 g of the mixed biomass was weighed using a digital balance and fed into the pyrolysis reactor. After loading, the reactor was tightly sealed, and all mechanical locks and condenser connections were secured to ensure airtight conditions.

The condenser tank was filled with water, and a continuous cooling system was established by regulating the inlet and outlet water flow to maintain a constant water level. Nitrogen (N_2) and LPG gas lines were connected, and leak checks were conducted prior to operation. The pyrolizer was then activated via the control panel, and the operating temperature was set to 500 °C. Nitrogen gas was introduced into the reactor at a low flow rate to create an inert atmosphere, followed by ignition of the LPG burner to initiate heating. The heating rate was monitored, and the time required to reach the target temperature was recorded.

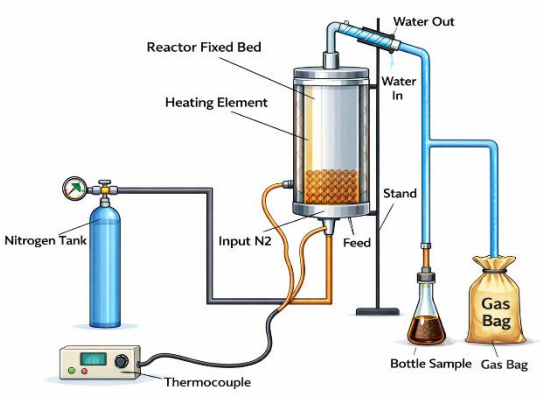

Figure 1. Schematic diagram of pyrolysis reactor.

Once the operating temperature of 500 °C was achieved, the pyrolysis process was maintained for 2 h. After completion, the nitrogen and LPG supplies were shut off, and all valves were closed. The bio-oil produced was collected and its volume was measured using a graduated Erlenmeyer flask. Schematic diagram of the pyrolysis reactor can be seen in Figure 1.

Phenolic Compound Extraction Process

The bio-oil was first neutralized using 2.5 M NaOH solution until a pH of 5 was achieved, as measured with a universal pH indicator. A volume of 6.5 mL of the neutralized bio-oil was then transferred into a three-neck round-bottom flask using a graduated pipette. Subsequently, 6.5 mL of 80% methanol and 6.5 mL of chloroform were added to the flask using separate graduated pipettes. The liquid–liquid extraction process was conducted for 60 min at the specified extraction temperature and stirring speed according to the experimental variables. After extraction, the resulting mixture was transferred to a separatory funnel and allowed to stand for 60 min to enable phase separation, forming the extract and raffinate phases.

Total Phenolic Compound Analysis by using Folin – Ciocalteu Method

The total phenolic compound (TPC) of the extract was determined using the Folin–Ciocalteu method. A 7.5% (w/v) Na_2CO_3 solution was prepared by dissolving 7.5 g of Na_2CO_3 in distilled water and diluting to a final volume of 100 mL. A 100 ppm gallic acid stock solution was prepared by dissolving 10 mg of gallic acid in distilled water and diluting to 100 mL. Calibration standards were prepared by transferring 0, 0.5, 1.0, 1.5, 2.0, 2.5, and 3.0 mL of the gallic acid stock solution into 10 mL volumetric flasks, followed by the addition of 0.5 mL of Folin–Ciocalteu reagent and thorough homogenization. Within 8 min, 4 mL of 7.5% Na_2CO_3 solution was added, and the mixture was diluted to volume with distilled water and homogenized. The solutions were allowed to stand for 105 min, after which the absorbance was measured at a wavelength of 765 nm using a UV–Vis spectrophotometer to generate a calibration curve ($y = mx + c$), where y represents absorbance and x represents gallic acid concentration.

For sample analysis, 1 mL of the extract or raffinate phase was transferred into a 10 mL volumetric flask, followed by the addition of 0.5 mL of Folin–Ciocalteu reagent and homogenization. Subsequently, 4 mL of Na_2CO_3 solution was added within 8 min, and the mixture was diluted to

volume with distilled water and homogenized. After standing for 105 min, the absorbance was measured at 765 nm using a UV–Vis spectrophotometer. The total phenolic content of the samples was determined from the calibration curve and expressed as gallic acid equivalents (GAE).

Thermodynamic Modelling of Liquid Liquid Equilibrium with NRTL Method

In general, the Non-Random Two-Liquid (NRTL) model is widely used to correlate equilibrium data in vapor–liquid and liquid–liquid equilibrium (LLE) systems. The presence of a non-randomness parameter in this model enables its application to a wide range of mixture systems and liquid–liquid equilibria by selecting an appropriate value of the parameter α. Furthermore, the NRTL model is capable of predicting equilibrium behavior in multicomponent systems without requiring additional adjustable parameters. The parameter α_{ij} represents the degree of non-randomness, which distinguishes the NRTL model from other activity coefficient models (Smith et al., 2001). In this study, the non-randomness parameter was assumed to be symmetric and set as shown in Eq. (1).

$$\alpha_{ij} = \alpha_{ji} = 0.3 \quad (1)$$

Many binary systems have been reported to exhibit α_{12} values in the range of 0.2–0.47. When experimental data are difficult to obtain, the value of α_{12} is commonly assumed, with $\alpha_{12} = 0.3$ being widely used as a reasonable approximation (Poling et al., 2001).

The interaction parameter τ_{ij} is defined as shown in Eq. (2).

$$\tau_{ij} = \frac{g_{ij} - g_{ji}}{RT} \quad (2)$$

where τ_{ij} represents the interaction parameter relating the binary interaction energies g_{ij} and g_{ji}, both of which are temperature-dependent and specific to each component pair. In this equation, R denotes the universal gas constant, and T is the absolute temperature in Kelvin. For non-ideal systems, temperature significantly influences the interaction terms in the NRTL model. For a binary system, three adjustable parameters are typically involved.

The term G_{ij} is defined as shown in Eq. (3).

$$G_{ij} = \exp(-\alpha_{ij}\tau_{ij}) \quad (3)$$

where G_{ij} represents the local composition contribution associated with components *i* and *j* at temperature *T*. The activity coefficient of each component can then be calculated using the Eqs. (4) – (6).

$$ln\gamma_i = \frac{\sum_{j=1}^{n}\tau_{ij}G_{ij}x_j}{\sum_{k=1}^{n}G_{ik}x_k} + \sum_{j=1}^{n} x_i \frac{G_{ij}x_j}{\sum_{k=1}^{n}G_{ik}x_k}\left(\tau_{ij} - \sum_{k=1}^{n}\frac{x_j\tau_{jk}G_{jk}}{\sum_{k=1}^{n}G_{jk}x_{jk}}\right) \quad (4)$$

$$x_i = exp\frac{\sum_{j=1}^{n}\tau_{ij}G_{ij}x_j}{\sum_{k=1}^{n}G_{ik}x_k} + \sum_{j=1}^{n} x_i \frac{G_{ij}x_j}{\sum_{k=1}^{n}G_{ik}x_k}\left(\tau_{ij} - \sum_{k=1}^{n}\frac{x_j\tau_{jk}G_{jk}}{\sum_{k=1}^{n}G_{jk}x_{jk}}\right) \quad (5)$$

$$\gamma_i = exp\frac{\sum_{j=1}^{n}\tau_{ij}G_{ij}x_j}{\sum_{k=1}^{n}G_{ik}x_k} + \sum_{j=1}^{n} x_i \frac{G_{ij}x_j}{\sum_{k=1}^{n}G_{ik}x_k}\left(\tau_{ij} - \sum_{k=1}^{n}\frac{x_j\tau_{jk}G_{jk}}{\sum_{k=1}^{n}G_{jk}x_{jk}}\right) \quad (6)$$

where ln γ_i represents the natural logarithm of the activity coefficient corresponding to mole fractions x_i and y_i in a liquid–liquid equilibrium system. In this study, x_i denotes the mole fraction of component *i* in the extract phase, while y_i represents the mole fraction in the raffinate phase.

After completing the thermodynamic calculations, the agreement between experimental data and model predictions was evaluated using the root-mean-square deviation (RMSD) as shown in Eq. (7). A smaller RMSD value, approaching zero, indicates better agreement between the experimental results and the values predicted by the NRTL model for liquid–liquid equilibrium.

$$RMSD = \sqrt{\frac{\sum_{t=1}^{T}(y_i experiment - y_i calculated)^2}{T}} \quad (7)$$

Where T is the number of experimental data.

Thermodynamic Modelling of Liquid Liquid Equilibrium with UNIQUAC Method

In liquid–liquid equilibrium modelling using the UNIQUAC model, the parameters r_i and q_i are required. The parameter r_i represents the volume parameter of a pure component, while q_i denotes the surface area parameter of the pure component. Each component possesses distinct volume and surface area values, and these parameters are used to calculate fugacity coefficients and area fractions.

The UNIQUAC model accounts for both the molecular volume and surface area contributions of each pure component, making it particularly suitable for mixtures with significant

differences in molecular size. In addition, this model can be applied to predict both vapor–liquid and liquid–liquid equilibria in binary and multicomponent systems, using only binary interaction parameters. The values of r_i and q_i for each component are presented in Table 1.

Table 1. Molecular surface area and volume parameters for the UNIQUAC model

Component	r	Q
Phenol	3.55	2.68
Methanol	1.43	1.43
Chloroform	2.70	2.34
Water	0.92	1.40

(Tamura *et al*., 2000)

The molar excess Gibbs free energy of a mixture is expressed as the sum of a combinatorial contribution and a residual contribution, as shown in Eq. (8). Accordingly, the natural logarithm of the activity coefficient of component *i* is also divided into combinatorial and residual terms, as presented in Eq. (9).

$$g = g^C + g^R \quad (8)$$

$$ln\gamma_i = ln\gamma_i^C + ln\gamma_i^R \quad (9)$$

The effects of molecular size and shape differences among the components and is determined by the volume parameter (r_i) and surface area parameter (q_i) of each pure component can be seen in Eq. (10). The energetic interactions between unlike molecules and depends on the surface area fraction and the binary interaction parameters is shown in Eq. (11).

$$ln\gamma_i^C = ln\frac{\emptyset_i}{x_i} + \frac{z}{r}q_i ln\frac{\theta_i}{\emptyset_i} + l_i - \frac{\emptyset_i}{x_i}\sum_j x_j\, l_j \quad (10)$$

$$ln\gamma_i^R = q_i\left(1 - lns_i - \sum_j \theta_j \frac{\tau_{ij}}{s_j}\right) \quad (11)$$

The subscripts *i*, *j*, and *k* denote the component indices (*i, j, k = 1, 2, 3, …, N*).

The surface area fraction (θ_i) and volume fraction ($\emptyset_i$) are calculated using Eqs. (12) and (13), respectively, based on the mole fraction (x_i) and UNIQUAC structural parameters (r_i and q_i). The binary interaction parameters τ_{ij} and τ_{ji} are defined as exponential functions of the interaction energy parameters (u_{ij} and u_{ji}), temperature (T), and the universal gas constant (R), as shown in Eqs. (14) and (15). The parameter l_i, given in Eq. (16), incorporates the coordination number (z), which was set to 10, as commonly assumed in UNIQUAC applications.

$$\theta_i = \frac{q_i x_i}{\sum_j q_j x_j} \quad (12)$$

$$\emptyset_i = \frac{q_i x_i}{\sum_j q_j x_j} \quad (13)$$

$$\tau_{ij} = exp\left(-\frac{u_{ij}}{R \times T}\right) \quad (13)$$

$$\tau_{ji} = exp\left(-\frac{u_{ji}}{R \times T}\right) \quad (14)$$

$$l_i = \frac{z}{2}(r_i - q_i) - (r_i - 1) \quad (15)$$

Finally, the complete expression for the activity coefficient of component *i*, combining both combinatorial and residual contributions, is presented in Eq. (16). This formulation enables the UNIQUAC model to accurately describe liquid–liquid equilibrium behavior in both binary and multicomponent systems using only binary interaction parameters.

$$ln y_i = ln\frac{\emptyset_1}{\theta_1} + \frac{z}{2}q_1 ln\frac{\emptyset_1}{\theta_1} + l_1 - \frac{\emptyset_1}{\theta_1}\sum_j x_j l_j + q_1\left[\begin{matrix}1 - ln\left(\sum_{j=1}^{m}\theta_j\tau_{ji}\right) \\ -\sum_{j=1}^{m}\frac{\theta_j\tau_{ji}}{\sum_{k=1}^{m}\theta_k\tau_{kj}}\end{matrix}\right] \quad (16)$$

Thermodynamic Modelling of Liquid Liquid Equilibrium with UNIFAC Method

The UNIFAC (UNIversal Functional Activity Coefficient) model consists of two main contributions, namely the combinatorial contribution and the residual contribution. The combinatorial contribution represents the effects of molecular size and shape, while the residual contribution accounts for the energetic interactions among functional groups within the solution. Through this group-contribution approach, the UNIFAC model can be used to predict phase equilibria, such as vapor–liquid equilibrium (VLE) and liquid–liquid equilibrium (LLE), in multicomponent systems using only molecular structural information.

The equations employed in the UNIFAC model are presented below, where the parameters r_i and q_i are calculated as the sums of the group volume (R_k) and group surface area (Q_k) parameters, respectively.

In the UNIFAC (UNIversal Functional Activity Coefficient) model, the molar excess Gibbs free energy of a mixture is expressed as the sum of a combinatorial contribution and a residual contribution, as shown in Eq. (17). The combinatorial term (Eq. (18)) accounts for the effects of molecular size and shape, which arise from differences in the volume and surface area of the components in the mixture. In contrast, the residual term (Eq. (19)) represents the energetic interactions between functional groups present in the solution and is responsible for capturing non-ideal behavior.

$$g = g^C + g^R \tag{17}$$

$$g^C = \sum_i x_i \ln\frac{\Phi_i}{x_i} + 5\sum_i q_i x_i \ln\frac{\theta_i}{\Phi_i} \tag{18}$$

$$g^R = -\sum_i q_i x_i \ln\left(\sum_j \theta_i \tau_{ji}\right) \tag{19}$$

The volume fraction (Φ_i) and surface area fraction (θ_i) of component i are calculated using Eqs. (20) and (21), respectively, based on the mole fraction (x_i) and the structural parameters r_i and q_i. In the UNIFAC approach, these structural parameters are obtained from a group-contribution method, where the molecular volume parameter (r_i) and surface area parameter (q_i) are calculated as the sums of the contributions from each functional group present in the molecule, as given in Eqs. (22) and (23). Here, $v_k^{(i)}$denotes the number of functional groups k in component i, while $R_k$and $Q_k$represent the group volume and surface area parameters, respectively.

$$\Phi_i = \frac{x_i r_i}{\sum_j x_j r_j} \tag{20}$$

$$\theta_i = \frac{x_i q_i}{\sum_j x_j r_j} \tag{21}$$

$$r_i = \sum_k v_k^{(i)} R_k \tag{22}$$

$$q_i = \sum_k v_k^{(i)} Q_k \tag{23}$$

The interaction between functional groups is described by the group interaction parameter τ_{ji}, which is defined as an exponential function of the group interaction energy difference and temperature, as shown in Eq. (24), where R is the universal gas constant and T is the absolute temperature. The activity coefficient of component i is then calculated as the sum of its combinatorial and residual contributions, as expressed in Eq. (25).

$$\tau_{ji} = exp\left(-\frac{u_{ji} - u_{ii}}{RT}\right) \tag{24}$$

$$\ln\gamma_i = \ln\gamma_i^C + \ln\gamma_i^R \tag{25}$$

The combinatorial contribution to the activity coefficient, given in Eq. (26), depends on the parameters $J_i$and L_i, which represent the normalized volume and surface area fractions of component i and are defined in Eqs. (28) and (29), respectively. The residual contribution, presented in Eq. (27), accounts for the energetic interactions among functional groups and involves the parameter S_i, defined in Eq. (30).

$$\ln\gamma_i^C = 1 - J_i + \ln J_i - 5q_i\left(1 - \frac{J_i}{L_i} + \ln\frac{J_i}{L_i}\right) \tag{26}$$

$$\ln\gamma_i^R = q_i\left(1 - \ln s_i - \sum_j \theta_j \frac{\tau_{ij}}{s_j}\right) \tag{27}$$

$$J_i = \frac{r_i}{\sum_j r_j x_j} \tag{28}$$

$$L_i = \frac{q_i}{\sum_j q_j x_j} \tag{29}$$

$$S_i = \tau_{ij}\sum_l \theta_l \tag{30}$$

RESULTS AND DISCUSSION

Mole Fraction of Components in the Extract and Raffinate Phases from Phenolic Compound Extraction

This study investigated liquid–liquid equilibrium (LLE) in the extraction of phenolic compounds at extraction temperatures of 30 °C, 40 °C, and 50 °C from bio-oil produced via the pyrolysis of mixed biomass waste at 500 °C. The experimental data obtained were subsequently correlated using the NRTL, UNIQUAC, and UNIFAC thermodynamic models. These models were selected due to their applicability to liquid–liquid equilibrium systems, both binary and multicomponent, across a wide range of mixtures.

The mole fractions of the components in the extract and raffinate phases were calculated based on phenolic compound absorbance data obtained from UV–Vis spectrophotometric analysis. The extract phase consisted of phenol, methanol, chloroform, and water, while the raffinate phase contained phenol, methanol, chloroform, and bio-oil.

Table 2 presents the absorbance values of the extract phase obtained from UV–Vis analysis during phenol extraction at various extraction temperatures and stirring speeds. Meanwhile, Table 3 shows the absorbance values of the raffinate phase, along with the corresponding phenol concentration, mass, and extraction yield.

Based on the data presented in Tables 2 and 3, increasing the extraction temperature from 30 °C to 50 °C significantly enhanced the phenol yield. This improvement can be attributed to increased diffusivity and decreased solvent-phase viscosity, which promote higher mass transfer rates. However, excessively high temperatures may lead to thermal degradation of phenolic compounds, indicating the existence of an optimal extraction temperature. An increase in stirring speed also improved the phenol yield by reducing the interfacial diffusion layer thickness. Nevertheless, once a critical stirring speed (plateau) was reached, no significant yield enhancement was observed, and excessively high stirring speeds increased the risk of emulsification (Fardhyanti, Imani, et al., 2020; Getachew et al., 2022).

Table 4 summarizes the calculated mole fractions of the four components in both the extract and raffinate phases at different extraction temperatures. Subsequently, the obtained mole fraction can be used in the calculation.

Liquid–Liquid Equilibrium Modelling of Phenolic Compound Extraction from Bio-Oil

This study evaluated liquid–liquid equilibrium (LLE) in a system consisting of phenol, methanol, chloroform, and water at extraction temperatures of 30 °C, 40 °C, and 50 °C. The experimental data obtained were subsequently

Table 2. Extract absorbance in phenol extraction using UV–Vis spectrophotometry

Extraction Temperature (°C)	Stirring Speed (rpm)	Absorbance	Concentration (mg/g)	Phenol Volume	Density (g/mL)	Mass
30	150	3.729	819.00	9.76	1.05	10.25
30	200	3.886	853.20	8.77	1.05	9.21
30	250	3.693	811.15	9.64	1.05	10.13
40	150	4.000	878.04	8.86	1.05	9.30
40	200	3.910	858.43	8.30	1.05	8.72
40	250	3.915	859.52	9.92	1.05	10.41
50	150	3.876	851.02	7.39	1.05	7.76
50	200	3.900	856.25	9.26	1.05	9.73
50	250	3.635	798.52	9.23	1.05	9.69

Table 3. Raffinate absorbance in phenol extraction using UV–Vis spectrophotometry

Extraction Temperature (°C)	Stirring Speed (rpm)	Absorbance	Concentration (mg/g)	Phenol Volume	Density (g/mL)	Mass	*Yield* (%)
30	150	4.11	902.22	4.73	1.05	4.96	67.37
30	200	3.87	849.06	3.84	1.05	4.03	69.56
30	250	3.78	830.98	4.35	1.05	4.56	68.94
40	150	3.82	839.48	3.16	1.05	3.32	73.68
40	200	4.04	887.41	3.20	1.05	3.36	72.15
40	250	3.74	821.83	3.54	1.05	3.72	73.69
50	150	3.83	841.66	2.38	1.05	2.50	75.62
50	200	4.17	915.29	3.23	1.05	3.39	74.14
50	250	3.83	839.91	3.17	1.05	3.32	74.46

.

Tabel 4. Mole fraction in the phenolic compound extraction process.

Temperature	Extract				Raffinate			
	x_a	x_b	x_c	x_d	y_a	y_b	y_c	y_d
	0.7	0.137	0.086	0.077	0.856	0.082	0.052	0.01
30	0.749	0.114	0.072	0.064	0.784	0.123	0.078	0.015
	0.688	0.142	0.09	0.08	0.76	0.137	0.086	0.017
	0.787	0.097	0.061	0.054	0.771	0.131	0.082	0.016
40	0.757	0.111	0.07	0.062	0.835	0.094	0.059	0.011
	0.759	0.11	0.069	0.062	0.748	0.144	0.091	0.018
	0.746	0.116	0.073	0.065	0.774	0.129	0.081	0.016
50	0.754	0.112	0.071	0.063	0.874	0.072	0.045	0.009
	0.671	0.15	0.095	0.084	0.772	0.13	0.082	0.016

Where,

x_a Mole fraction of phenol in the extract phase
x_b: Mole fraction of methanol in the extract phase
x_c: Mole fraction of chloroform in the extract phase
x_d: Mole fraction of water in the extract phase
y_a: Mole fraction of phenol in the raffinate phase
y_b: Mole fraction of methanol in the raffinate phase
y_c: Mole fraction of chloroform in the raffinate phase
y_d: Mole fraction of water in the raffinate phase

correlated using the NRTL, UNIQUAC, and UNIFAC thermodynamic models. These models were selected due to their applicability to liquid–liquid equilibrium systems, both binary and multicomponent, over a wide range of mixture types. It is expected that the correlations obtained from these models can be used for interpolation and extrapolation of phase equilibrium behavior in this system.

Interaction Parameters from NRTL, UNIQUAC, and UNIFAC Modeling

The experimental data were correlated using the NRTL and UNIQUAC equations. In determining the fitting parameters for the NRTL model, the non-randomness parameter (α) must first be specified. For liquid–liquid equilibrium systems involving polar and non-polar mixtures, the value of α generally falls within the range of 0.2–0.47. In this study, a value of α = 0.3 was employed, as it represents a commonly used and recommended value in the literature (Poling et al., 2001).

For parameter estimation using the UNIQUAC model, the molecular surface area (q) and molecular volume (r) parameters of each component were first determined. The interaction parameters for the NRTL and UNIQUAC models used in the calculations are presented in Table 5. Subgroup parameter for UNIFAC model can be seen in Table 6.

Determination of Activity Coefficient Values from Phenolic Compound Extraction Calculations Using the NRTL, UNIQUAC and UNIFAC Methods

Tables 7–9 present the activity coefficient values obtained for the phenol extraction process using methanol and chloroform as solvents, as calculated using the NRTL, UNIQUAC, and UNIFAC models.

In general, activity coefficients are closely related to phase equilibrium, the law of mass action, and Gibbs free energy. In thermodynamics, activity coefficients are used to describe the deviation of a mixture from ideal behavior. When the activity coefficient (γ) equals 1, the component behaves ideally; values of γ > 1 or γ < 1 indicate positive or negative deviations from Raoult's law, respectively. A negative deviation indicates that the component is more volatile. When ln γ is positive, the process proceeds spontaneously toward the products, whereas a negative ln γ indicates spontaneous phases. A similar trend is observed in the UNIQUAC model, where phenol again exhibits the most ideal behavior among the components. Likewise, calculations based on the UNIFAC model indicate that phenol has an activity coefficient value closest to unity, confirming that it is the most ideal component in the system.

Table 5. Interaction parameter from the NRTL and UNIQUAC model.

Temperature (°C)	Component (i-j)	NRTL Parameter		UNIQUAC Parameter	
		gij	gji	uij	uji
30	1-2	7903	4655	728	1003
	1-3	0	28794	62478	43
	1-4	12792	13732	3	2338
	2-3	6573	3990	202841	50681
	2-4	9495	10315	76912	38
	3-4	12641	524	29038	18509
40	1-2	8482	7553	0	455
	1-3	0	8323	62479	39
	1-4	13709	15624	3	2505
	2-3	9510	0	202841	50681
	2-4	10550	6086	76912	37
	3-4	9798	505	29036	63623
50	1-2	9059	6458	0	439
	1-3	0	31750	62479	39
	1-4	13185	15784	3	2514
	2-3	10339	3226	202841	50681
	2-4	10309	3317	76912	37
	3-4	9183	594	29036	63623

Where component (1) Phenol; (2) Methanol; (3) Chloroform and (4) Water

Tabel 6. UNIFAC subgroup parameters.

Main Group	Subgroup	k	Rk	Qk	Examples of molecules and their constituent groups	
1 "CH_2"	CH_3	1	0.9011	0.848	n-Butane:	$2CH_3$, $2CH_2$
	CH2	2	0.6744	0.540	Isobutane:	$3CH_3$, 1CH
	CH	3	0.4469	0.228	2,2-Dimethyl propane:	$4CH_3$, 1C
	C	4	0.2195	0.000		
3 "ACH" (AC = aromatic carbon)	ACG	19	0.5313	0.400	Benzene:	6ACH
4"$ACCH_2$"	$ACCH_3$	12	1.2663	0.968	Toluene:	5ACH, $1ACCH_3$
	$ACCH_2$	13	1.0496	0.660	Ethylbenzene:	$1CH_3$, 5ACH, $1ACCH_2$
5 "OH"	OH	15	1.0000	1.200	Ethanol:	$1CH_3$, $1CH_2$, 1OH
7 "H_2O"	H_2O	17	0.9200	1.400	Water:	$1H_2O$
9"CH_2CO"	CH_3CO	19	1.6724	1.488	Acetone:	$1CH_3CO$, $1CH_3$
	CH_2CO	20	1.4457	1.180	3-Pentanone:	$2CH_3$, $1CH_2CO$, $1CH_2$
13"CH_2O"	CH_3O	25	1.1450	1.088	Dimethyl ether:	$1CH_3$, $1CH_3O$
	CH_2O	26	0.9183	0.780	Diethyl ether:	$2CH_3$, $1CH_2$, $1CH_2O$
	CH-O	27	0.6908	0.468	Diisopropyl ether:	$4CH_3$, 1CH, 1CH–O
15 "CNH"	CH_3NH	32	1.4337	1.244	Dimethylamine:	$1CH_3$, $1CH_3NH$
	CH_2NH	33	1.2070	0.936	Diethylamine:	$2CH_3$, $1CH_2$, $1CH_2NH$
	CHNH	34	0.9795	0.624	Diisopropylamine:	$2CH_3$, $1CH_2$, $1CH_2NH$
19 "CCN"	CH_3CN	41	1.8701	1.724	Acetonitrile:	$1CH_3CN$
	CH_2CN	42	1.6434	1.416	Propionitrile	$1CH_3$, $1CH_2CN$

(Smith *et al*., 2016)

Table 7. Coefficient of activity calculated by NRTL method

Temperature (°C)	Extract				Raffinate			
	γ_a^I	γ_b^I	γ_c^I	γ_d^I	γ_a^{II}	γ_b^{II}	γ_c^{II}	γ_d^{II}
	1.324	9.086	17916.529	43.447	1.084	15.184	29725.841	299.016
30	1.228	10.962	21773.389	57.548	1.177	10.252	20113.768	236.127
	1.349	8.752	17151.391	40.895	1.216	9.129	17821.165	216.689
	1.180	18.069	3.020	70.391	1.207	13.512	2.241	227.884
40	1.229	15.998	2.679	56.139	1.116	18.935	3.181	310.806
	1.227	16.143	2.700	56.241	1.245	12.268	2.057	203.789
	1.263	14.277	33451.610	51.613	0.967	0.914	0.911	3.939
50	1.248	14.751	34580.335	54.401	0.865	1.614	1.603	5.943
	1.415	11.441	26281.909	33.057	0.865	1.132	1.152	6.128

Table 8. Coefficient of activity calculated by UNIQUAC method

Temperature (°C)	Extract				Raffinate			
	γ_a^I	γ_b^I	γ_c^I	γ_d^I	γ_a^{II}	γ_b^{II}	γ_c^{II}	γ_d^{II}
	0.101	0.280	0.139	0.609	0.083	0.253	0.121	0.579
30	0.095	0.271	0.133	0.598	0.091	0.266	0.129	0.598
	0.102	0.283	0.141	0.612	0.093	0.270	0.132	0.604
	1.180	18.069	3.020	70.391	0.092	0.268	0.131	0.601
40	1.229	15.998	2.679	56.139	0.085	0.257	0.124	0.585
	1.227	16.143	2.700	56.241	0.094	0.272	0.133	0.606
	0.095	0.271	0.133	0.598	0.091	0.267	0.130	0.600
50	0.094	0.270	0.132	0.596	0.082	0.251	0.119	0.575
	0.104	0.285	0.143	0.615	0.092	0.267	0.130	0.600

Table 9. Coefficient of activity calculated by UNIFAC method.

Temperature (°C)	Extract				Raffinate			
	γ_a^I	γ_b^I	γ_c^I	γ_d^I	γ_a^{II}	γ_b^{II}	γ_c^{II}	γ_d^{II}
	0.992	1.006	1.295	2.859	0.856	0.082	0.052	0.010
30	0.994	1.016	1.256	2.830	1.000	1.069	1.075	0.307
	0.991	1.004	1.305	2.872	1.000	1.071	1.073	0.308
	0.992	1.006	1.295	2.859	1.000	1.070	1.074	0.307
40	0.994	1.016	1.256	2.830	1.000	1.065	1.080	0.307
	0.991	1.004	1.305	2.872	1.000	1.072	1.072	0.308
	0.994	1.015	1.259	2.829	1.000	1.070	1.074	0.308
50	0.995	1.016	1.253	2.826	1.000	1.062	1.083	0.309
	0.989	1.001	1.318	2.883	1.000	1.070	1.074	0.307

Where,

γ_a^I : Coefficient activity of phenol in extract
γ_b^I : Coefficient activity of methanol in extract
γ_c^I : Coefficient activity of chloroform in extract
γ_d^I : Coefficient activity of water in extract
γ_a^{II} : Coefficient activity of phenol in raffinate
γ_b^{II} : Coefficient activity of methanol in raffinate
γ_c^{II} : Coefficient activity of chloroform in raffinate
γ_d^{II} : Coefficient activity of water in raffinate

progression toward the reactants. A value of ln γ = 0 signifies that the system has reached equilibrium.

The results calculated using the NRTL model show that phenol is the component closest to ideal behavior in both the extract and raffinate

The consistency of phenol activity coefficients approaching unity is in good agreement with the low RMSD values obtained for the NRTL model, indicating superior predictive accuracy of this model compared to the UNIQUAC and UNIFAC models in describing the liquid–liquid equilibrium behavior of the system.

Relationship Between Experimental Data and Calculated Data in NRTL, UNIQUAC, and UNIFAC Modeling

The calculated results and experimental data obtained were subsequently correlated using the NRTL, UNIQUAC, and UNIFAC models and are presented in graphical form in Figure 2.

Figure 2 illustrates the comparison of mole fractions in the extract and raffinate phases obtained from the extraction of bio-oil produced by the pyrolysis of biomass waste at 500 °C, between

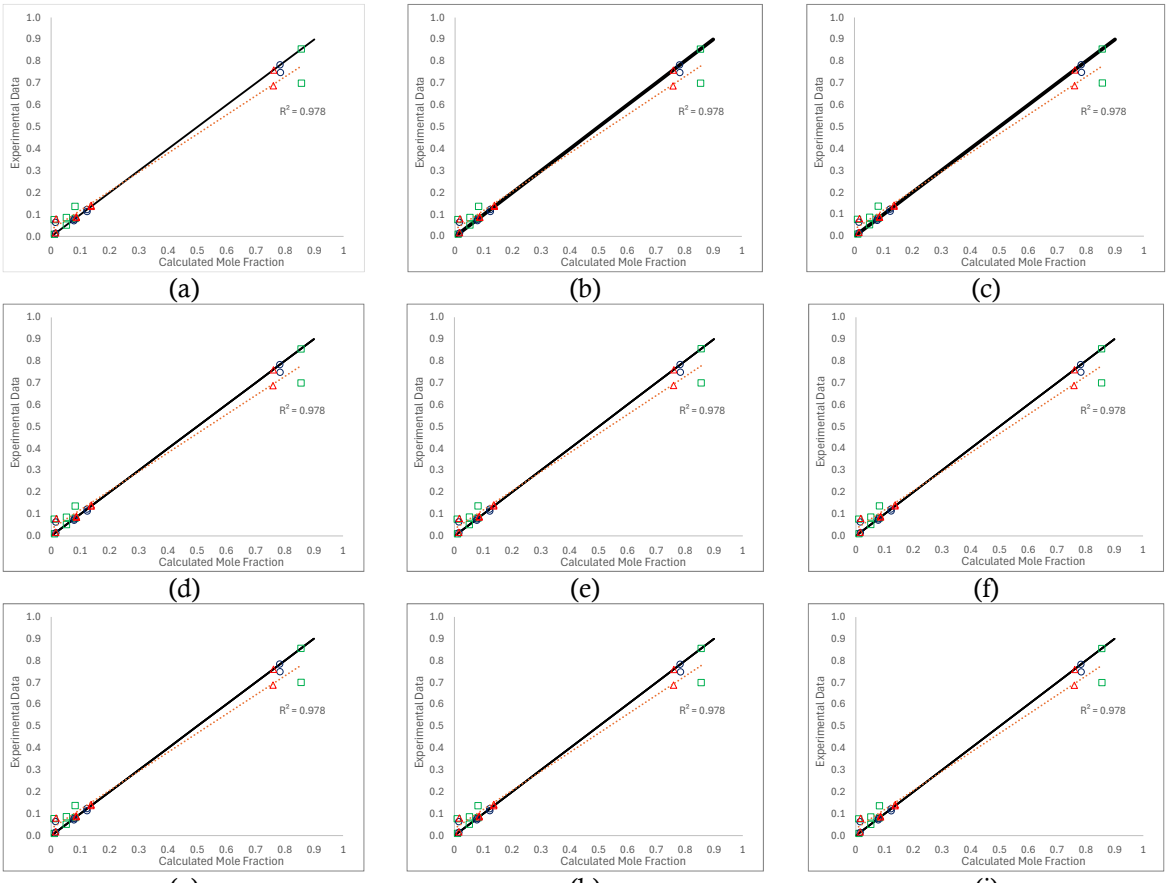

Figure 2. Relationship between experimental data and calculated data using the NRTL model at extraction temperatures of (a) 30°C, (b) 40°C and (c) 50°C (c); the UNIQUAC model at extraction temperatures of (d) 30°C, (e) 40°C and (f) 50°C; and the UNIFAC model at extraction temperatures of (g) 30°C, (h) 40°C and (i) 50°C.

experimental data and calculated results using the NRTL, UNIQUAC, and UNIFAC models. Visually, Graphs B, E, and H exhibit the closest agreement with the linear reference line. Based on the comparison between experimental and calculated data for phenolic compound extraction from bio-oil at extraction temperatures of 30 °C, 40 °C, and 50 °C, the results closest to the linear trend were observed at an extraction temperature of 40 °C.

Correlation of the liquid–liquid equilibrium data using the NRTL model demonstrates good agreement between experimental results and calculated values. This finding is consistent with previous studies reported by Ferdinal and Wibowo (2021).

Error Evaluation in the Calculations

Based on Table 10, the correlation results indicate that the NRTL, UNIQUAC, and UNIFAC equilibrium models can be applied to predict liquid–liquid equilibrium (LLE) in the phenol extraction process from bio-oil produced by the pyrolysis of mixed biomass waste using methanol and chloroform as solvents, with good accuracy as evidenced by RMSD values below 1%. A smaller RMSD value indicates better agreement between experimental data and calculated results.

Tabel 10. RMSD values.

Temperature (°C)	RMSD (%)		
	NRTL	UNIQUAC	UNIFAC
30	0.0438	0.045828	0.0627
40	0.0259	0.02794	0.0446
50	0.0400	0.04191	0.0505

Based on both the visual comparison in Figure 2 and the RMSD values in Table 10, the NRTL model provides the most optimal performance for modelling liquid–liquid equilibrium in phenol extraction at an extraction temperature of 40 °C from bio-oil derived from the pyrolysis of mixed biomass waste at 500 °C. The NRTL model incorporates a non-randomness parameter (α), which allows the equation to be applied to various types of mixtures and liquid–liquid equilibrium systems by selecting an appropriate α value. The NRTL equation is capable of representing both vapor–liquid and liquid–liquid equilibria in binary and multicomponent systems using only binary interaction parameters. In addition, its formulation is relatively simpler than those of the UNIQUAC and UNIFAC models and often provides superior results, particularly for dilute systems.

CONCLUSION

Extraction temperature significantly influences the liquid–liquid equilibrium (LLE) behavior in the phenol extraction process from bio-oil derived from the pyrolysis of mixed biomass waste when modeled using the NRTL, UNIQUAC, and UNIFAC equations. Among the investigated temperatures, an extraction temperature of 40 °C provided the most consistent and reliable equilibrium correlations. Phenol was identified as the component closest to ideal behavior in both the extract and raffinate phases, as indicated by activity coefficient values approaching unity across all three thermodynamic models. This behavior confirms the suitability of the selected solvent system (methanol–chloroform) for phenol extraction from bio-oil. Increasing extraction temperature from 30 °C to 50 °C enhanced phenol yield, primarily due to increased diffusivity and reduced solvent viscosity, which improved mass transfer. However, the results also indicate the existence of an optimal temperature range, as excessively high temperatures may promote phenolic compound degradation and reduce separation efficiency. Stirring speed positively affected phenol recovery by reducing interfacial mass transfer resistance. Nevertheless, beyond a critical stirring speed, further increases did not significantly improve. Overall, the results demonstrate that the NRTL model is the most appropriate thermodynamic model for predicting liquid–liquid equilibrium in the phenol extraction process from bio-oil produced by pyrolysis of mixed biomass waste at 500 °C, and it can be reliably used for process design, interpolation, and extrapolation purposes.

ACKNOWLEDGMENTS

Authors would like to acknowledge the Universitas Negeri Semarang for providing the fund through DPA UNNES 2025.

REFERENCES

Dolah, R., Karnik, R., Hamdan, H. 2021. A comprehensive review on biofuels from oil palm empty bunch (EFB): Current status, potential, barriers and way forward. Sustainability. 13(18): 10210.

Fardhyanti, D. S., Chafidz, A., Triwibowo, B., Prasetiawan, H., Cahyani, N. N., Andriyani, S. 2020. Improving the Quality of Bio-oil Produced from Rice Husk Pyrolysis by Extraction of its Phenolic Compounds. Jurnal Bahan Alam Terbarukan. 8(2): 90–100.

Fardhyanti, D. S., Imani, N. A. C., Damayanti, A., Mardhotillah, S. N., Afifudin, M., Mulyaningtyas, A., Akhir, A. E., Nuramalia, W., Maulana, P. 2020. The separation of phenolic compounds from bio-oil produced from pyrolysis of

corncobs. AIP Conference Proceedings. 2243.

Fardhyanti, D. S., Megawati, Kurniawan, C., Sigit Lestari, R. A., Triwibowo, B. 2018. Producing *Bio-oil* from Coconut Shell by Fast Pyrolysis Processing. MATEC Web of Conferences. 237: 2001.

Fathahillah, I., Islam, H., Widyastuti, R. W., Nugraha, A., Pratama, R., Purniawan, A. 2022. Antasena Biohidrogen: Generator Berbasis Limbah Kelapa Sawit Guna Meningkatkan Kerja Sama Indonesia-Tiongkok Di Bidang Renewable Energy. OISAA Journal of Indonesia Emas. 5(1): 43–56.

Febriyanti, F., Fadila, N., Susandy, A., Yazid Bindar, S., Irawan, A. 2019. Pemanfaatan Limbah Tandan Kosong Kelapa Sawit Menjadi Bio-Char, Bio-Oil Dan Gas Dengan Metode Pirolisis. Jurnal Chemurgy. 3(2): 12–17.

Ferdinal, M. F., Wibowo, A. A. 2021. Studi Optimasi Pressure Swing Distillation Pada Pemurnian Etanol Menggunakan CHEMCAD. Jurnal Teknologi Separasi. 7(2): 255–263.

Getachew, A. T., Holdt, S. L., Meyer, A. S., Jacobsen, C. 2022. Effect of Extraction Temperature on Pressurized Liquid Extraction of Bioactive Compounds from Fucus vesiculosus. Marine Drugs. 20(4): 263.

Gufron, M., Hairul Bahri, M., Fathonisyam, A. P. 2023. Analisis Kadar Air, Densitas Bulk dan Pembakaran pada Pelet Biomassa Ampas Tebu Variasi Ukuran Partikel dan Penambahan Bahan Aditif (Zeolit, Karbon Aktif). Jurnal Smart Teknologi. 4(2): 2774–1702.

Hertadi, C. D. P., Sulaiman, M., Anwar, P. G. P. 2022. Kajian Industri Energi Terbarukan Tenaga Listrik di Indonesia Berdasarkan Arah Kebijakan dan Potensi Alam. G-Tech: Jurnal Teknologi Terapan. 6(2): 276–283.

Kumar, R., Strezov, V., Weldekidan, H., He, J., Singh, S., Kan, T., Dastjerdi, B. 2020. Lignocellulose biomass pyrolysis for bio-oil production: A review of biomass pre-treatment methods for production of drop-in fuels. Renewable and Sustainable Energy Reviews. 123: 109763.

Lestari, I., Anggorowati, H., Hadi, F. 2021. Efek Pretreatment Ultrasonikasi Terhadap Hidrolisis Enzimatis Spirulina platensis Residue. EKSERGI. 18(1): 24–28.

Logayah, D. S., Mustikasari, B. R., Zahra Hindami, D., Rahmawati, R. P. 2023. Krisis Energi Uni Eropa: Tantangan dan Peluang dalam Menghadapi Pasokan Energi yang Terbatas. Hasanuddin Journal of International Affairs. 3(2): 2775–3336.

López, H. D., Ayala, N., Malagón-Romero, D. 2021. Evaluation of the Production of Bio-oil Obtained Through Pyrolysis of Banana Peel Waste. Chemical Engineering Transactions. 89: 637–642.

Mora-Villalobos, J. A., Aguilar, F., Carballo-Arce, A. F., Vega-Baudrit, J. R., Trimino-Vazquez, H., Villegas-Peñaranda, L. R., Stöbener, A., Eixenberger, D., Bubenheim, P., Sandoval-Barrantes, M., Liese, A. 2023. Tropical agroindustrial biowaste revalorization through integrative biorefineries—review part I: coffee and palm oil by-products. Biomass Conversion and Biorefinery. 13(2): 1469–1487.

Ordonez-Loza, J., Chejne, F., Jameel, A. G. A., Telalovic, S., Arrieta, A. A., Sarathy, S. M. 2021. An investigation into the pyrolysis and oxidation of bio-oil from sugarcane bagasse: Kinetics and evolved gases using TGA-FTIR. Journal of Environmental Chemical Engineering. 9(5): 106144.

Poling, B. E., Prausnitz, J. M., O'connell, J. P. 2001. The Properties Of Gases And Liquids Fifth Edition (Vol. 5). McGraw-Hill Education.

Prastika, A. 2023. Hubungan Antara Tingkat Konsumsi Energi Listrik dengan Pertumbuhan Ekonomi di Indonesia. Jurnal Ilmu Ekonomi (JIE). 7(1): 18–29.

Putri, D. R., Khoirunnisa, S., Widiyanto, A. 2023. Peningkatan Keterampilan Warga Desa Purwojiwo dalam Pembuatan Bahan Bakar Briket Sebagai Upaya Pemanfaatan Limbah Pertanian Bonggol Jagung. Jurnal Bina Desa. 5(1): 119–123.

Putri, R. W., Nurisman, E. 2019. Produksi bio-oil dari limbah kulit durian dengan proses pirolisis lambat. Jurnal Teknik Kimia. 25(2): 50–53.

Smith, J. M., Van Ness, H. C., Abbott, M. M., Swihart, M. T. 2016. Chemical

Engineering Thermodynamics (8th ed.). McGraw-Hill Education.

Statistics, T. G. 2023. Indonesia Population Statistics 2025 | Current Population. The Data Expert. https://www.theglobalstatistics.com/indonesia-population-statistics. Accessed at 25 January 2025.

Tamura, K., Chen, Y., Tada, K., Yamada, T., Nagata, I. 2000. Representation of Multicomponent Liquid-Liquid Equilibria for Aqueous and Organic Solutions Using a Modified UNIQUAC Model. Journal of Solution Chemistry. 29(5): 463-488.

Yudhistira, F. H., Wibowo, A. A. 2022. Green Diesel: Bahan Bakar Cair Terbarukan Pengganti Biodiesel. Distilat. 8(4): 979–987.

Zhu, Y., Xu, G., Song, W., Zhao, Y., Miao, Z., Yao, R., Gao, J. 2021. Catalytic microwave pyrolysis of orange peel: Effects of acid and base catalysts mixture on products distribution. Journal of the Energy Institute. 98: 172–178.